Histol Histopathol (2025) 40: 477-483

Histology and Histopathology
From Cell Biology to Tissue Engineering

ORIGINAL ARTICLE Open Access

Collagen fiber arrangement in the normal bladder lamina propria and their potential impact on the pathological substaging of bladder cancer stage T1

Ofer N. Gofrit[1], Vladimir Yutkin[1], Mordechai Duvdevani[1], Guy Hidas[1] and Tzahi Neuman[2]

[1]Department of Urology and [2]Department of Pathology, Hadassah Hebrew University Hospital, Jerusalem, Israel

Summary. The lamina propria (LP) of the urinary bladder lies between the urothelial mucosa and the muscularis propria. This complex stratum is composed of extracellular matrix, several cell types, and collagen types I and III fibers. LP invasion by urothelial carcinoma (progression from stage Ta to T1) is a determinant of bladder cancer advancement. We attempted to characterize collagen fiber arrangement in the LP. This could enrich our understanding of this important layer and potentially provide clues for sub-staging of the T1 bladder cancer. A total of 24 Masson trichrome-stained images of normal bladder, including 12,530 collagen fibers were quantitatively analyzed using the Dragonfly software. The LP was divided according to fiber orientation into superficial LP (SLP, 15% of the thickness) and the deep LP (DLP, 85% of the thickness). Collagen fiber geometry analysis demonstrated that the SLP fibers are more parallel to the urothelium with an average angle of 26°±23° compared to 40°±26° in the DLP ($p=3.4x10^{-144}$), more packed (average distance to the closest fiber of 0.61±0.67 compared to 0.66±0.77, p=0.0001), and their aspect ratio is considerably longer (average of 1.93±0.12 compared to 0.20±0.11, $p=2.84x10^{-8}$). No difference was found in fiber perimeter or Feret diameter. Thus, we conclude that bladder collagen fibers are arranged in two distinct layers: a dense-ordered SLP and a loose disorder DLP. This indicates that the physical barrier to cancer cell invasion probably lies in the SLP, immediately underneath the urothelium. Once this barrier is breached, the looser and disorganized DLP poses no remarkable obstacle. Thus, we believe that histology-based subdivisions of stage T1 are expected to fail in providing clinically meaningful prognostic information.

Key words: Urinary bladder, Lamina propria, Collagen fibers

Introduction

"There is nothing in this world that does not have a decisive moment."

Cardinal de Retz

The bladder urothelium lies on a 50-100-nm-thick basement membrane. This dense, amorphous, sheet-like structure is comprised of collagen type IV and several proteoglycans, including laminin and heparan sulfate. It is secreted and maintained by the urothelium itself (Kalluri et al., 2003). The lamina propria (LP) underlines the basement membrane. It is composed of the extracellular matrix, several cell types including fibroblasts, adipocytes, immune cells and collagen fibrils (approximately 70% is type I and 30% is type III) produced by fibroblasts. The LP is rich in blood vessels, lymphatic channels, and sensory nerve endings. Close to the muscularis propria, the LP gradually becomes more loose allowing for some mobility (Reuter and Al-Ahmadie, 2015). Light and electron microscopy reveals the presence of delicate discontinuous smooth muscle fascicles in the middle of the LP, the muscularis mucosa (MM) (Dixon and Gosling, 1983).

The fourth and eighth most common cancer in men and women, respectively, is bladder cancer (BC) (Siegel et al., 2023). It arises in the urothelium, and 70–80% of the tumors fails to invade further (stage Ta). Tumor cells breaching into the LP (stage T1) degrade it via the matrix metalloproteinase (secreted by tumor cells themselves or stimulated by epithelial or stromal

Corresponding Author: Dr. Ofer N. Gofrit, Department of Urology Hadassah University Hospital, P.O.Box 12000, Jerusalem 91120, Israel. e-mail: ogofrit@gmail.com

www.hh.um.es. DOI: 10.14670/HH-18-817

Abbreviations. LP, lamina propria; MM, muscularis mucosa; SLP, superficial lamina propria; DLP, deep lamina propria; TURBT, transurethral resection of the bladder tumor; BC, bladder cancer; TEM, transmission electron microscope

cells) by applying physical force and by piercing contracting filopodia (Song et al., 2022). Stage Ta to T1 progression is a "Retz type" decisive moment in cancer evolution toward higher stages leading to lymphatic invasion and metastases. When a T1 tumor is found in transurethral resection of the bladder tumor (TURBT), the risk of understaging is high. Thus, most authorities recommend a "second look" TURBT. Muscularis propria invasion (stage T2) can then be found in up to 40% of the cases. After the initial resection (and the "second look"), the risk of T1 tumor recurrence is still high at approximately 69% to 80%. Moreover, there is also a 30% to 50% risk of progression to stage T2 or beyond within 5 years (Nepples and O'Donnell, 2009). Obviously, early radical cystectomy can cure T1 BC; however, most patients do not accept this mutilative surgery knowing that it would eventually be overtreatment in 50–70%. Patients with T1 cancer are thus trapped in a dilemma between missing the window of cure and avoiding overtreatment. This problem fuels the search for prognostic markers that can reliably predict which T1 BC will progress. Histological subdivision of stage T1 was proposed as potential markers.

Several stage T1 subdivisions were proposed, the majority of which rely on the identification of the MM. These include three subdivisions: superficial, into, and deep to the MM, as substages T1a, T1b, and T1c or the two-subdivision superficial or deep to the MM as stages T1a and T1b (Younes et al., 1990; Hasui et al., 1994; Holmäng et al., 1997; Herman et al., 1998; Kondyls et al., 2000; Bernadini et al., 2001; Orsola et al., 2005; Rouprêt et al., 2012). All studies demonstrated predictive information. However, due to dependence on tissue orientation and difficulties in identifying the MM in many cases, the current staging system categorizes all tumors invading the LP as T1 without subdivisions (AJCC, 6th ed, 2002).

This study aimed to characterize the collagen morphology of the normal urinary bladder LP through computerized analysis. This information is important from a histologic point of view and can potentially provide a useful model for T1 substaging.

Materials and methods

Patients and imaging capture

The study is based on an analysis of 24 normal bladder specimens obtained from 18 patients (16 men and 2 women) with a mean age 69.0 years (SD 13.2 years). The specimens were random bladder biopsies obtained for various reasons, at a distance of at least 2 cm away from the main pathology. Patients' demographics and final diagnoses are shown in Table 1. The major pathology of all patients was bladder cancer at various stages and grades except one patient that had a completely normal bladder (biopsies were done in his case to rule out interstitial cystitis). All hematoxylin and eosin-stained (H&E) slides were reviewed by a dedicated uropathologist (TN), and their normality was approved. The paraffin-embedded blocks were stained with Masson trichrome staining (Trichrome Staining Kit, Roche). A specimen with a relatively straight epithelium was captured using an Olympus Camedia digital camera connected to an Olympus microscope, under ×200 magnifying objective.

Tissue for Transmission electron microscope (TEM) was fixed in a solution containing 2% paraformaldehyde, 2.5 % gluteraldehyde EM grade, in 0.1M sodium cacodylate buffer pH 7.3 for 2 hours at RT followed by 24 hours at 4°C. The tissue was then washed 4 times with sodium cacodylate and postfixed for 1h with 1% osmium tetroxide, 1.5% potassium ferricyanide in sodium cacodylate, and washed 4 times with the same buffer, followed by dehydration with graded series of ethanol solutions (30, 50, 70, 80, 90, 95 %) for 10 minutes each and then 100% ethanol 3 times for 20 minutes each, followed by 2 changes of propylene oxide. The tissue was then infiltrated with series of epoxy resin, (25,50, 75, 100%) 24 hours each and polymerized in the oven at 60°C for 48 hours. The blocks were sectioned by an ultramicrotome (Ultracut E, Riechert-Jung), and sections of 80 nm were obtained and stained with uranyl acetate and lead citrate. Sections were observed by Jeol 1400 Plus TEM at ×1500 and ×3000 magnifications.

The study was approved by the local IRB (HMO-0567-23) that waived the requirement for informed consent.

Image analysis

The bladder LP is composed of easily recognized two layers, the superficial LP (SLP) and deep LP (DLP),

Table 1. Patients' demographics and final diagnoses.

Slide Number	Gender	Age	Final diagnosis
1,2	M	27	Normal bladder
3,4	M	72	TaLG
5,6	M	54	TaLG
7	M	65	TaLG
8	M	76	T1HG
9	M	56	TaLG
10	M	77	T2HG
11	M	66	T1HG
12,13	M	73	T1HG
14,15	M	75	T1HG
16	M	77	T1HG
17,18	M	78	T2HG
19	F	75	T1HG
20	M	74	T1HG
21	F	87	TaLG
22	M	75	T1HG
23	M	71	T1HG
24	M	65	TaHG
Average		69.0	
STDEV		13.2	

with a seemingly different collagen arrangement. This can be well appreciated on H&E staining (Fig. 1). With Masson trichrome, the difference is even more prominent (Fig. 2, Supplementary Material 1). Detection of collagen fibers and quantitative image analysis of their parameters were performed with the Dragonfly software on bright field. To get clean images of the collagen fibers and not to count nuclei as fibers, the Dragonfly algorithm excludes the nuclei. This is done according to the aspect ratio (AR). AR is the ratio between object's width and length. The AR of a perfect circle is 1. Lower ARs mean noncircular objects. The algorithm is designed to remove all objects with AR>0.9, i.e., nuclei. Next, the algorithm detects and segments fibers according to a defined color range and automatically calculates their lengths and orientations. The parameters evaluated were the number of collagen fibers, fiber angle axis in relation to the urothelium (defined as 0°), fiber perimeter, fiber aspect ratio, fiber Feret diameter (longest projection), and fiber distant to the closest object (another collagen fiber). Statistical comparisons of SLP and DLP were performed using a two-tailed t-test with Microsoft excel software. A p-value <0.05 was considered statistically significant. Analysis of collagen fibril orientation in TEM was qualitative.

Results

Masson trichrome

A total of 12,530 collagen fibers were found on the 24 images analyzed. The relative thickness of the superficial and deep layers is presented in Table 2, and the morphological analysis in Table 3. The SLP included 2734 fibers and occupied approximately 15% of the LP thickness and the DLP included 9797 fibers and occupied approximately 85% of the thickness. The most notable differences between the SLP and DLP were in fiber angle axis in relation to the urothelium (Fig. 3). Average angle of the SLP fibers was 26° (±23°) compared to 40° (±26°) in the DLP ($p=3.4\times10^{-144}$). The SLP fibers were significantly more packed (average distance to the closest fiber of 0.61±0.67 compared to 0.66±0.77 (p=0.0001), and their aspect ratio was significantly longer (average of 1.93±0.12 compared to 0.20±0.11, $p=2.84\times10^{-8}$). No differences were found in the fiber perimeter or fiber Feret diameter.

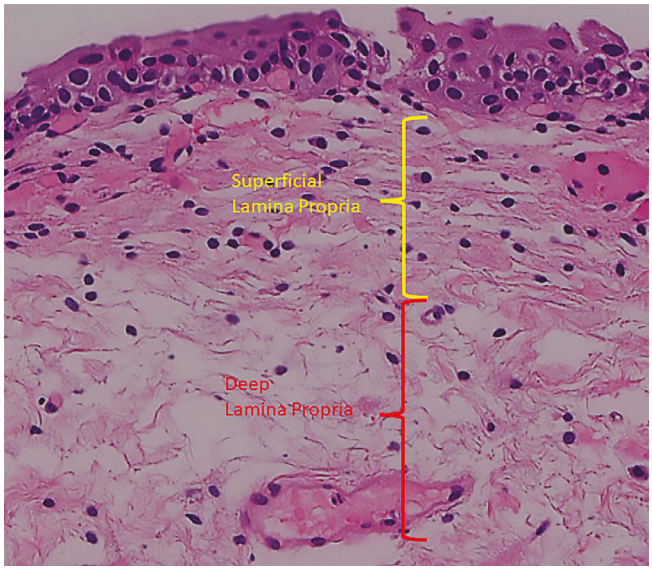

Fig. 1. Biopsy of a normal bladder. The biopsy was obtained from a 45-year-old woman suspected of suffering from interstitial cystitis. This diagnosis was not supported by this biopsy. Collagen fiber arrangement is different in the superficial and deep aspects of the LP. H&E. x 200

Transmission electron microscope (TEM) findings

Representative TEM photos of a normal bladder mucosa obtained from a 71- year-old man with benign prostatic hyperplasia are shown in Fig. 4. SLP collagen fibrils exhibit a tight and parallel pattern compared to their disorganized pattern in the DLP. This analysis is qualitative.

Discussion

The deeper aspect of the bladder LP is composed of

Table 2. The relative thickness of the superficial and deep layers of the normal bladder.

Slide number	SLP* %	DLP*%	SLP/SLP+DLP%	DLP/SLP+DLP%
1	32	118	0.213333333	0.786666667
2	16	150	0.096385542	0.903614458
3	11	95	0.103773585	0.896226415
4	19	150	0.112426036	0.887573964
5	29	105	0.21641791	0.78358209
6	20	155	0.114285714	0.885714286
7	16	100	0.137931034	0.862068966
8	19	130	0.127516779	0.872483221
9	20	100	0.166666667	0.833333333
10	12	135	0.081632653	0.918367347
11	30	85	0.260869565	0.739130435
12	25	84	0.229357798	0.770642202
13	24	112	0.176470588	0.823529412
14	20	130	0.133333333	0.866666667
15	32	112	0.222222222	0.777777778
16	12	112	0.096774194	0.903225806
17	17	154	0.099415205	0.900584795
18	16	150	0.096385542	0.903614458
19	15	125	0.107142857	0.892857143
20	20	125	0.137931034	0.862068966
21	18	135	0.117647059	0.882352941
22	20	155	0.114285714	0.885714286
23	22	75	0.226804124	0.773195876
24	23	144	0.137724551	0.862275449
average	20.33333	122.3333	0.14694721	0.85305279
SD	5.961227	24.53333	0.053122192	0.053122192
median	20	125	0.130425056	0.869574944

*SLP: superficial lamina propria, DLP: deep lamina propria.

more loose connective tissue compared to its superficial aspect. This feature enables the bladder to form mucosal folds when contracted (Reuter and Al-Ahmadie, 2015). However, these differences were never quantified and are ignored in attempts to substage T1 BC. In this study, we found that the bladder LP is composed of two distinct layers via a computerized analysis of 12,530 Masson trichrome-stained collagen fibers: an ordered SLP which is significantly tighter and more parallel to the urothelium collagen fibers compared to the more

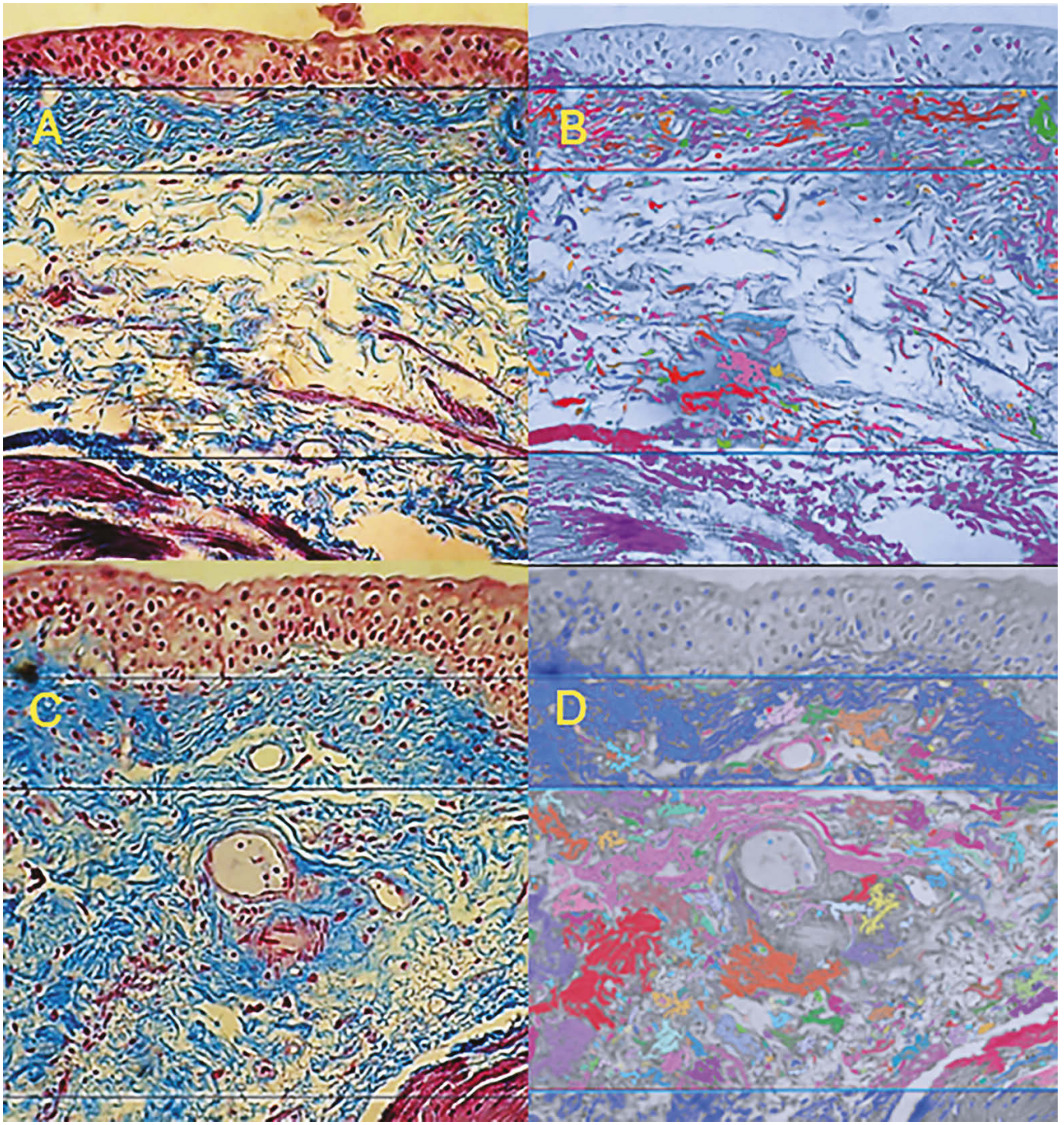

Fig. 2. Examples of Masson Trichrome stained normal bladder specimens analyzed with the Dragonfly software. **A, B.** A 66-year-old man with T1 high-grade tumor (#11). **C, D.** A 73-year-old man with T1 high-grade tumor #12. The rectangles represent the SLP and DLP.

disordered and looser DLP. The SLP comprises approximately 15% of LP thickness, while the DLP is 85% (Table 1, Figs. 1-3). These findings were also discernable at the fibrillar level by TEM (Fig. 4).

Most of the clinical interest in the architecture of the LP stems from attempts to render BC stage T1 less unpredictable. This disease has a risk of progression to potentially lethal stages in 30% to 50% of the patients (Nepples and O'Donnell, 2009). The mirror image of this is overtreatment in 50-70% of the patients if all T1 patients undergo radical cystectomy. Several attempts were made to identify T1 patients at high risk for progression according to the histological findings. The description of MM in about the middle of the LP opened the possibility of substaging T1 relative to the MM (Dixon and Gosling, 1983). Several investigators in the late 20th and early 21st centuries examined the prognostic value of MM-based subdivisions and found seemingly useful prognostic information. For example, Smits et al. reported stage progression (to ≥ T2) in 6%, 33%, and 55% of patients with T1a, T1b, and T1c, respectively ($p<0.001$) (Smits et al., 1998). Nevertheless, owing to difficulties in identifying the MM (in up to 40% of the specimens) and heavy dependence of these substaging systems on specimen orientation, MM-based subdivisions were mostly abandoned (Leivo et al., 2018). Moreover, from a biological point of view, imagining how an interrupted tiny smooth muscle cells poses any actual barrier to advancing tumor cells is difficult. The "statistically significant" findings reported in many MM-based subdivisions could have been a surrogate of more prognostically relevant parameters such as tumor burden.

Indeed, tumor-burden-based substaging systems were also proposed. Levio et al. examined the significance of linear length of invasion into the LP. They demonstrated that a cutoff of 2.3 mm provides potential prognostic significance (Leivo 2018). Additional burden-based staging was conducted by van Rhijn et al. (2012). These authors subdivided T1 to T1m (a single focus of LP invasion with a diameter of ≤0.5 mm) and T1e (multiple microinvasions or larger area of invasion) and demonstrated clinically useful information. However, this subclassification is also highly sampling and orientation-based method and harder for pathological standardization and implementation (due to the need for accurate measurements). Thus, the current TNM staging system failed to recognize any subdivision of stage T1 as clinically useful. It does, however, acknowledge that such subdivision would be welcome.

Interestingly, thus far, the potential prognostic information embodied in the arrangement of collagen fibers in the LP has been ignored. In other malignancies, this is well recognized. In breast cancer, tumor cells change collagen fibril orientation in the LP while still confined to epithelium, and this can possibly facilitate invasion. This phenomenon is classified according to tumor-associated collagen signature (TACS) types. In TACS 1, collagen fibrils underlying the tumor become denser. In TACS 2, collagen fibrils align in parallel to the tumor boundary, and in TACS 3, the fibrils align perpendicular to the tumor boundary (Provenzano et al., 2006; Song et al., 2022). The presence of TACS 3 is an independent prognostic indicator associated with a significantly worse disease-specific survival (Conklin et al., 2011). Oriented collagen fibrils can also assist in angiogenesis by steering angiogenic sprouts into the tumor (Song et al., 2022).

The current study underscored collagen architecture

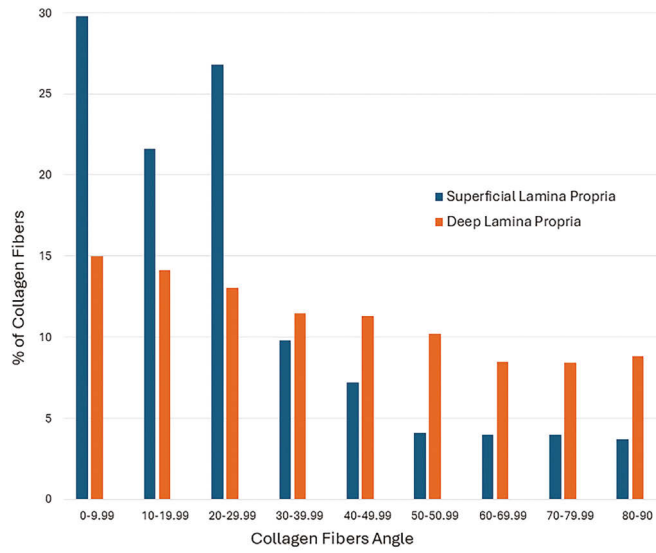

Fig. 3. Histogram showing collagen fiber angle axis relative to the urothelium (defined as 0^0). Collagen fibers of the superficial lamina propria show smaller angles (more parallel to the epithelium) compared to fibers in the deep lamina propria.

Table 3. Morphological parameters of the superficial lamina propria (SLP), the deep lamina propria (DLP), and both layers. Statistical comparisons of SLP and DLP was done with a two tailed t-test.

	Average angle to urothelium (SD)	Average perimeter (SD)	Average aspect Ratio (SD)	Average Feret Diameter (SD)	Average distance to closest Object (SD)
SLP	26.0° (23.08°)	11.62 (65.28)	1.93 (0.12)	1.99 (4.67)	0.61 (0.67)
DLP	39.66° (26.01°)	21.58 (250.05)	0.20 (0.12)	2.00 (4.36)	0.67 (0.80)
Total LP	36.69° (26.01°)	19.4 (223.24)	0.20 (0.11)	2.00 (4.43)	0.66 (0.77)
p value	$3.4x10^{-144}$	0.08	$2.84x10^{-8}$	0.96	0.0001

of the normal bladder. Unfortunately, its arrangement, with the densely packed fibers just beneath the urothelium, indicates that the physical barrier of the LP is at the superficial layer. A tumor that managed to cross this barrier will face no further physical obstacles deeper. The effect of low and high-grades superficial urothelial cancer (Ta) and CIS of bladder on its underlying LP should be the target of further studies employing this methodology, and so do the effects of benign conditions such as inflammation. Moreover, the LP contains multiple components in addition to collagens, including extracellular matrix, and many cell types. Their complex interplay with the cancer cells can also provide insights into the biology of cancer invasion.

This study is limited by sample size, by male predominance, and by the patients' relatively older age. A similar study in younger population or in a predominantly female population may yield different results. However, BC, the source of interest in the LP substructure, is prevalent in the population studied here. Furthermore, in this study, most of the specimens were obtained from the dome and lateral walls of the bladder. The exact origin of each specimen was not recorded and differences in the architecture of different locations could account for some of SDs in Table 1. Additionally, the bladder trigone is generally not sampled (to avoid damage to the ureteral orifices), and therefore, collagen arrangement in the trigone or bladder neck could be different.

Conclusions

In this work, we elucidated that collagen fibers of the normal bladder LP are arranged in two distinct layers, a dense and parallel SLP and a loose and disordered DLP. Considering their architecture, it is highly reasonable that the barrier to the advancing tumor cells lies in the SLP, immediately underneath the urothelium. Once this layer is crossed, no additional physical barriers in the DLP will be observed. Since this

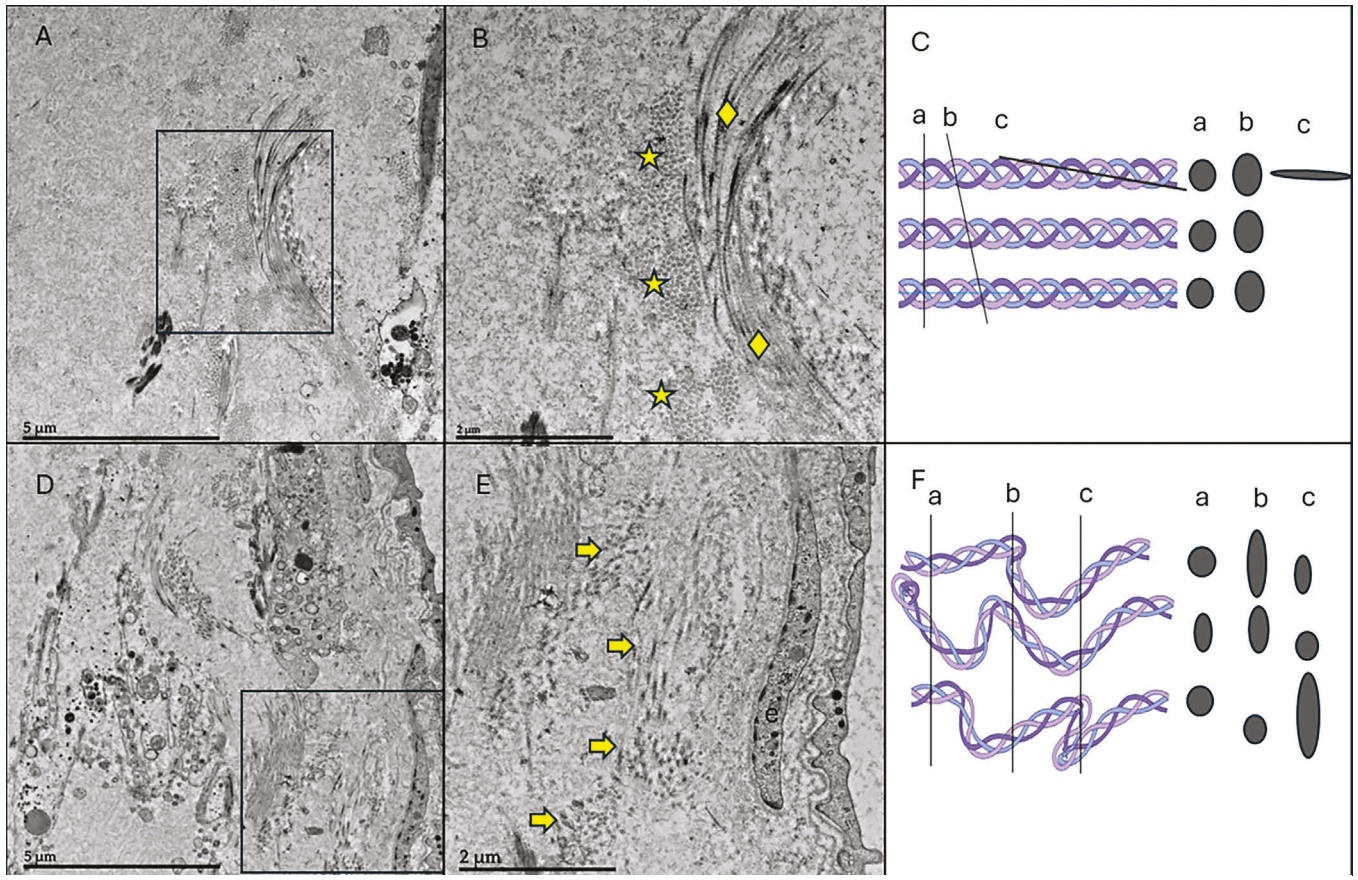

Fig. 4. Representative TEM photos of a normal bladder (71-year-old man, slice width 80 nm). **A-C.** Superficial lamina propria. **A.** The black rectangle demonstrates the region portrayed in panel **B** Parallel collagen fibrils are observed, with some perpendicular (asterisk) and some longitudinal (rhombus). **C.** Graphical depiction of parallel fibrils cut at different angles. Every angle shows different widths; however, in each orientation, the fibrillar diameter is similar. **D-F.** Deep lamina propria. **D.** The black rectangle shows the region portrayed in panel **E** (×3000, e-endothelial cell). Nonparallel collagen fibrils (arrows) show collagen fibrils with different diameters. **F.** Graphical depiction of nonparallel fibrils cut at various angles. Fibrils with different widths are observed. Scale bars: A, D, 5 μm; B, E, 2 μm.

physical barrier is in the most superficial stratum of the LP, we assume that morphology-based subdivisions of stage T1 are expected to fail. The methodology described here can be employed in evaluating other organs and can potentially modify our view of their histology.

Acknowledgements. Dr. Itay Spektor from "Histospeck, Histology and Image Analysis", Tel-Aviv, analyzed the Masson trichrome images.
Msc. Hava Glickstein from the Electron Microscopy Unit, The Core Research Facility, The Hebrew University-Hadassah Medical School, Ein Kerem performed the TEM studies.
The study was not supported by extra-institutional funding.
Conflict of interest. None.

References

Bernardini S., Billerey C., Martin M., Adessi G.L., Wallerand H. and Bittard H. (2001). The predictive value of muscularis mucosae invasion and p53 over expression on progression of stage T1 bladder carcinoma. J. Urol. 165, 42-46.

Conklin M.W., Eickhoff J.C., Riching K.M., Pehlke C.A., Eliceiri K.W., Provenzano P.P. and Friedl A. and Keely P.J. (2011). Aligned collagen is a prognostic signature for survival in human breast carcinoma. Am. J. Pathol. 178, 1221-1232.

Dixon J.S. and Gosling J.A. (1983). Histology and fine structure of the muscularis mucosae of the human urinary bladder. J. Anat. 136, 265-271.

Greene F.L., Page D.L., Fleming I.D., Fritz A.G., Blach C.H., Haller D.G. and Morrow M. (2002). AJCC Cancer Staging Manual. 6th ed. Springer Science+Business Media New York. pp 335-341.

Hasui Y., Osada Y., Kitada S. and Nishi S. (1994). Significance of invasion to the muscularis mucosae on the progression of superficial bladder cancer. Urology 43, 782-786.

Hermann G.G., Horn T. and Steven K. (1998). The influence of the level of lamina propria invasion and the prevalence of p53 nuclear accumulation on survival in stage T1 transitional cell bladder cancer. J. Urol. 159, 91-94.

Holmäng S., Hedelin H., Anderström C., Holmberg E. and Johansson S.L. (1997). The importance of the depth of invasion in stage T1 bladder carcinoma: a prospective cohort study. J. Urol. 157, 800-803.

Kalluri R. (2003). Basement membranes: structure, assembly and role in tumour angiogenesis. Nat. Rev. Cancer 3, 422-433.

Kondylis F.I., Demirci S., Ladaga L., Kolm P. and Schellhammer P.F. (2000). Outcomes after intravesical bacillus Calmette-Guerin are not affected by substaging of high grade T1 transitional cell carcinoma. J. Urol. 163, 1120-1123.

Leivo M.Z., Sahoo D., Hamilton Z., Mirsadraei L., Shabaik A., Parsons J.K., Kader A.K., Derweesh I., Kane C. and Hansel D.E. (2018). Analysis of T1 bladder cancer on biopsy and transurethral resection specimens: Comparison and ranking of T1 quantification approaches to predict progression to muscularis propria invasion. Am. J. Surg. Pathol. 42, e1-e10.

Nepple K.G. and O'Donnell M.A. (2009). The optimal management of T1 high-grade bladder cancer. Can. Urol. Assoc. J. 3 (6 Suppl 4), S188-192.

Orsola A., Trias I., Raventós C.X., Español I., Cecchini L., Búcar S., Salinas D. and Orsola I. (2005). Initial high-grade T1 urothelial cell carcinoma: Feasibility and prognostic significance of lamina propria invasion microstaging (T1a/b/c) in BCG-treated and BCG-non-treated patients. Eur. Urol. 48, 231-238.

Paner G.P., Stadler W.M., Hansel D.E., Montironi R., Lin D.W. and Amin M.B. (2018). Updates in the eighth Edition of the tumor-node-metastasis staging classification for urologic cancers. Eur. Urol. 73, 560-569.

Provenzano P.P., Eliceiri K.W., Campbell J.M., Inman D.R., White J.G. and Keely P.J. (2006). Collagen reorganization at the tumor-stromal interface facilitates local invasion. BMC Med. 26, 38.

Reuter V.E. and Al-Ahmadie H. (2015). Urothelial Tract: Renal pelvis, ureter, urinary bladder and urethra In: Sternberg's Diagnostic Surgical Pathology. 6th ed. Mills S.E. (ed). Wolters Kluwer pp. 957-958.

Rouprêt M., Seisen T., Compérat E., Larré S., Mazerolles C., Gobet F., Fetissof F., Fromont G., Safsaf A., d'Arcier B.F., Celhay O., Validire P., Rozet F., Irani J., Soulié M. and Pfister C. (2013). Comité de Cancérologie de l'Association Française d'Urologie. Prognostic interest in discriminating muscularis mucosa invasion (T1a vs T1b) in nonmuscle invasive bladder carcinoma: French national multi-center study with central pathology review. J. Urol. 189, 2069-2076.

Siegel R.L., Miller K.D., Wagle N.S. and Jemal A. (2023). Cancer statistics, 2023. C.A. Cancer J. Clin. 73, 17-48.

Smits G., Schaafsma E., Kiemeney L., Caris C., Debruyne F. and Witjes J.A. (1988). Microstaging of pT1 transitional cell carcinoma of the bladder: identification of subgroups with distinct risks of progression. Urology 52, 1009-1013.

Song K., Yu Z., Zu X., Li G., Hu Z. and Xue Y. (2022). Collagen re-modeling along cancer progression providing a novel opportunity for cancer diagnosis and treatment. Int. J. Mol. Sci. 23, 10509.

van Rhijn B.W., van der Kwast T.H., Alkhateeb S.S., Fleshner N.E., van Leenders G.J., Bostrom P.J., van der Aa M.N., Kakiashvili D.M., Bangma C.H., Jewett M.A. and Zlotta A.R. (2012). A new and highly prognostic system to discern T1 bladder cancer substage. Eur. Urol. 61, 378-384.

Younes M., Sussman J. and True L.D. (1990). The usefulness of the level of the muscularis mucosae in the staging of invasive transitional cell carcinoma of the urinary bladder. Cancer 66, 543-548.

Accepted September 19, 2024